

Thorax

CTAS - A CT score to quantify disease activity in pulmonary sarcoidosis

Journal:	Thorax
Manuscript ID	thoraxjnl-2016-208833.R1
Article Type:	Research Letter
Date Submitted by the Author:	n/a
Complete List of Authors:	Benamore, Rachel; Oxford University Hospitals NHS Trust, Radiology Kendrick, Yvonne; Weatherall Institute of Molecular Medicine, MRC Human Immunology Unit repapi, emmanouela; Weatherall Institute of Molecular Medicine, Computational Biology UNit Helm, Emma; University Hospitals Coventry and Warwickshire NHS Trust, Department of Radiology cole, suzanne; Weatherall Institute of Molecular Medicine, MRC Human Immunology Unit taylor, stephen; Weatherall Institute of Molecular Medicine, Computational Biology Unit Ho, Ling-Pei; Weatherall Institute of Molecular Medicine, MRC Human Immunology Unit; Churchill Hospital, Oxford Centre for Respiratory Medicine
Keywords:	Sarcoidosis, Imaging/CT MRI etc

SCHOLARONE™
Manuscripts

CTAS - A CT score to quantify disease activity in pulmonary sarcoidosis

Rachel Benamore^{1*}, Yvonne R. Kendrick^{2,5*}, Emmanouela Repapi³, Emma Helm⁴,
Suzanne L Cole⁵, Stephen Taylor³, and Ling-Pei Ho^{2,5} * *Equal first authors.*

¹Thoracic Imaging Department
Churchill Hospital, Oxford OX3 7LJ

²Oxford Interstitial Lung Disease Service
Oxford Centre for Respiratory Medicine
Churchill Hospital, Oxford OX3 7LJ

³Computational Biology Research Group
Weatherall Institute of Molecular Medicine
University of Oxford OX3 9DS

⁴University Hospitals Coventry and Warwickshire NHS Trust
Clifford Bridge Road
Coventry CV2 2DX

⁵MRC Human Immunology Unit
Weatherall Institute of Molecular Medicine
University of Oxford OX3 9DS

Correspondence to

Ling-Pei Ho
Oxford Interstitial Lung Disease Service,
Churchill Hospital, Oxford OX3 7LJ
Email - Ling-pei.ho@imm.ox.ac.uk

ABSTRACT

Background A major gap in the management of sarcoidosis is the lack of accessible and objective methods to measure disease activity. Since 90% of patients have pulmonary involvement, we explored if a disease activity score based on thoracic CT scans could address this clinical issue.

Methods. High resolution CT scans from 100 consecutive sarcoidosis patients at a regional sarcoidosis service were scored for extent of CT abnormalities known to relate to granuloma or lymphocytic infiltration from published CT-pathological studies. These individual abnormality scores were then correlated against serum ACE, sIL-2R and change in forced vital capacity (FVC) to identify CT abnormalities that reflect contemporaneous disease activity. The sum of these scores, or **CT Activity Score** (CTAS) was then validated against FVC response to treatment.

Findings CT extent scores for nodularity, ground-glass opacification, inter-lobular septal thickening and consolidation correlated significantly with at least one of the disease activity parameters and were used to form CTAS. CTAS was found to predict FVC response to treatment at one year and was highly reproducible between radiologists. An abbreviated CTAS (aCTAS), constructed from presence or absence of the four CT abnormalities also showed significant correlation with FVC response to treatment. CTAS and aCTAS also correlated with response to treatment in the fibrotic subgroup.

Interpretation CTAS provides a concept for an objective and reproducible CT scoring method to quantify disease activity in sarcoidosis. The score can potentially be used to stratify patients according to disease activity, determine response to treatment and establish if fibrotic sarcoidosis is active.

1
2
3
4
5
6
7
8
9
10
11
12
13
14
15
16
17
18
19
20
21
22
23
24
25
26
27
28
29
30
31
32
33
34
35
36
37
38
39
40
41
42
43
44
45
46
47
48
49
50
51
52
53
54
55
56
57
58
59
60

A major gap in the management of sarcoidosis is the lack of accessible and objective methods to measure disease activity¹. This has contributed to difficulties in deciding when treatment should be started or discontinued particularly in fibrotic disease, and has hampered the evaluation of costly treatments such as biologics or cytokine modulators. The most commonly reported end point in clinical trials for pulmonary sarcoidosis is change in lung function measurements. However, this does not detect reduction in disease activity after treatment, which, in sarcoidosis, can also occur without change in lung function.

90% of patients with sarcoidosis have pulmonary involvement, and high resolution computed tomographic (HRCT) scan of the lung is performed in nearly all patients for diagnostic purposes. In addition, CT-pathological studies have shown that typical abnormalities like broncho-vascular nodularity, ground glass opacity and consolidation correlate to presence of granuloma on open lung biopsies²⁻⁴. Nodularity also associates strongly with bronchoalveolar lavage (BAL) cell count and serum soluble IL-2 receptor (sIL-2R) levels⁴, and profusion of interlobular septal thickening correlates with BAL lymphocytosis⁵. We therefore explored if systematically measuring these HRCT abnormalities would allow quantification of disease activity in pulmonary sarcoidosis.

100 consecutive patients with pulmonary sarcoidosis from the Oxford Sarcoidosis Service who had HRCT scan performed from 2011, and fulfilling the diagnostic criteria proposed by WASOG were recruited. All patients were followed up for one year to record change in treatment and lung function. The study was approved by the South Central National Research Ethics Service committee. Detailed study methods are found in Supplementary Methods.

Thoracic HRCT scan and full pulmonary function testing were performed within 4 weeks of each other for all patients. Each HRCT was specifically scored for the presence, character and extent of sarcoidosis-related HRCT abnormalities [ground glass opacification (GGO), interlobular septal thickening (IST), nodularity, conglomeration, consolidation and intra-thoracic lymphadenopathy] using pre-defined criteria from either the Fleischner Society glossary of terms or pre-defined criteria from previous peer-reviewed publications (Supplementary Table 1-3). In an unselected proportion of patients - serum sIL-2R levels (n=21); serum ACE (n=72) and lung function at baseline and 12 months after CT scan (regardless of treatment) (n=40) were also performed. These parameters were used to reflect active macrophage and granuloma, T cell activity, and overall disease activity. FVC change was measured as % change over a year from baseline, to represent disease reversibility and therefore, a surrogate of activity.

Scoring of the HRCT scans was performed by a Fellowship-trained Consultant Thoracic Radiologists (RB). To evaluate reproducibility of the final composite score, the first 85 scans were selected for scoring by a second radiologist based at a district general hospital (EH).

97 patients had complete CT analyses. Demographic data and specific clinical characteristics are shown in Table 1. 100% of patients had intra-thoracic lymphadenopathy, 33% showed presence of GGO, 73% nodularity, 34% IST, 24% conglomeration and 20% consolidation (further details in Supplementary Table 4). Thirty-four (35%) patients showed evidence of fibrosis. Four patients had evidence of pulmonary hypertension on CT scan, confirmed on right heart pressure assessment by echocardiography.

1
2
3
4
5
6
7
8
9
10
11
12
13
14
15
16
17
18
19
20
21
22
23
24
25
26
27
28
29
30
31
32
33
34
35
36
37
38
39
40
41
42
43
44
45
46
47
48
49
50
51
52
53
54
55
56
57
58
59
60

Extent scores for nodularity, IST, consolidation and GGO but not conglomeration or lymphadenopathy correlated with at least one of the surrogate of disease activity (Supplementary Table 5). Based on these findings, we excluded conglomeration and lymphadenopathy and took the sum of the scores of GGO, IST, consolidation and nodularity as the composite score for disease activity. We termed this the 'CT Activity Score' or 'CTAS'. The CTAS score in our cohort ranged from 0 to 58, with a median of 10 (IQR 0-19) (Supplementary Figure 1a). Fibrotic patients had higher CTAS compared to non-fibrotic [(median of 15.8 (IQR 8.5-22.0) vs 9.8 (4.0-15.0); $p<0.001$, Mann-Whitney test] (Supplementary Figure 1b); and CTAS was higher with worse lung function (Supplementary Figure 1c-e). Examples of CT scans showing divergent CTAS are shown in Supplementary Figure 2.

To provide a validation of the relationship of CTAS to disease activity, we examined if CTAS was able to predict the size of response to treatment. We reasoned that if CTAS reflected disease activity, then, the higher the CTAS value, the greater the ability of lung function (FVC) to improve with treatment. Twenty-nine patients went on to start or increase treatment specifically for their lung disease within four weeks of HRCT scanning. FVC values at 12 months (± 8 weeks) after treatment were compared to pre-treatment. We found that CTAS predicted the size of FVC response to treatment at one year [$b=0.42$ (C.I. 0.05-0.79); $r^2=0.17$, $p=0.03$] (Figure 1a). This was also the case for the fibrotic subgroup, where 20 of the 34 patients received treatment [$b=0.32$ (C.I. 0.0-0.6); $r^2=0.20$, $p=0.04$](Figure 1b).

Comparing the CTAS to any one CT parameter (GGO, nodularity, consolidation and IST), we found only GGO and consolidation to predict treatment response ($p=0.04$ and 0.05 respectively), and at a weaker certainty than CTAS ($p=0.03$). Therefore the composite measure of CTAS provides the strongest correlation with FVC response after treatment.

We also examined an abbreviated CTAS (aCTAS) comprising the sum of presence (1) or absence (0) of each of the four CT feature (GGO, nodularity, IST and consolidation) and found that this produced similar correlation outcomes to CTAS for lung function and response to treatment (Figure 1 c-d and Supplementary Figure 1f-h).

We found a strong correlation between radiologists for the CTAS ($r = 0.91$; $p < 0.0001$; Pearson's correlation test; $n=85$), and Bland-Altman analysis confirmed that there was no systematic deviation in measurements over the range of values (Supplementary Figure 3). There was no difference in aCTAS between the two radiologists ($r = 1.0$; $n=85$).

We propose CTAS as a promising concept for measurement of disease activity in pulmonary sarcoidosis. Our study was limited in size but is the first description of a numerical CT score for extent of disease activity in pulmonary sarcoidosis. The validation component was limited to patients who were started on treatment during the year ($n=29$) and will benefit from further evaluation with a bigger cohort. Measurements of disease severity on HRCT (but not activity) have been previously published⁷⁻¹⁰. CTAS is specifically designed to reflect the extent of disease activity regardless of the level of lung function impairment and fibrosis. Indeed, CTAS and aCTAS could be particularly useful in aiding decisions on whether to treat fibrotic sarcoidosis. A CT scan showing volume loss and established fibrosis has often been termed 'burnt out' fibrosis but may contain areas of active disease that may be driving the fibrotic process. We propose that a conclusion of 'active' or 'inactive' disease (with aCTAS), based on the absence or presence of any of these four CT abnormalities could be a useful addition to an HRCT report for pulmonary sarcoidosis. A validation study will strengthen and possibly refine the score and provide an opportunity to bring this score into clinical practice.

REFERENCES

1. Valeyre D, Prasse A, Nunes H, Uzunhan Y, Brillet PY, Müller-Quernheim J. Sarcoidosis. *Lancet Respir Med.* 2014;383(9923):1155-67.

2. Spagnolo P, Sverzellati N, Wells AU, Hansell DM. Imaging aspects of the diagnosis of sarcoidosis. *Eur Radiol.* 2014;24(4):807-16.

3. Leung AN, Brauner MW, Caillat-Vigneron N, Valeyre D, Grenier P. Sarcoidosis activity: correlation of HRCT findings with those of 67Ga scanning, bronchoalveolar lavage, and serum angiotensin-converting enzyme assay. *Journal of Computer Assisted Tomography.* 1998;22(2):229-34.

4. Nishimura K, Itoh H, Kitaichi M, Nagai S, Izumi T. Pulmonary sarcoidosis: correlation of CT and histopathologic findings. *Radiology.* 1993;189(1):105-9.

5. Nishimura K, Itoh H, Kitaichi M, Nagai S, Izumi T. CT and pathological correlation of pulmonary sarcoidosis. *Semin Ultrasound CT MR.* 1995;16(5):361-70.

6. Oberstein A, von Zitzewitz H, Schweden F, Muller-Quernheim J. Non invasive evaluation of the inflammatory activity in sarcoidosis with high-resolution computed tomography. *Sarcoidosis, Vasculitis, and Diffuse Lung Diseases* 1997;14(1):65-72.

7. Remy-Jardin M, Giraud F, Remy J, Wattinne L, Wallaert B, Duhamel A. Pulmonary sarcoidosis:role of CT in the evaluation of disease activity and functional impairment and in prognosis assessment. *Radiology.* 1994;191(3):675-80.

8. Drent M, De Vries J, Lenters M, Lamers RJ, Rothkranz-Kos S, Wouters EF, et al. Sarcoidosis: assessment of disease severity using HRCT. *European Radiology.* 2003;13(11):2462-71.

9. Zappala CJ, Desai SR, Copley SJ, Spagnolo P, Sen D, Alam SM, et al. Accuracy of individual variables in the monitoring of long-term change in pulmonary sarcoidosis as judged by serial high-resolution CT scan data. *Chest.* 2014;145(1):101-7.

10. Prasse A, Katic C, Germann M, Buchwald A, Zissel G, Müller-Quernheim J. Phenotyping sarcoidosis from a pulmonary perspective. *Am J Respir Crit Care Med* 2008; 177: 330–36.

FIGURE LEGENDS

Figure 1. Association between CTAS and aCTAS and changes in FVC at 12 months in patients who received new or increased treatment after CT scan, for all patients (A and C), and for the fibrotic subgroup (B and D). r and p values shown are from linear regression calculations. Spearman Correlation values are (A-B) $r=0.40$, $p=0.03$ and $r=0.35$, $p=0.13$; and (C-D) $r=0.42$, $p=0.02$ and $r=0.34$, $p=0.13$ respectively.

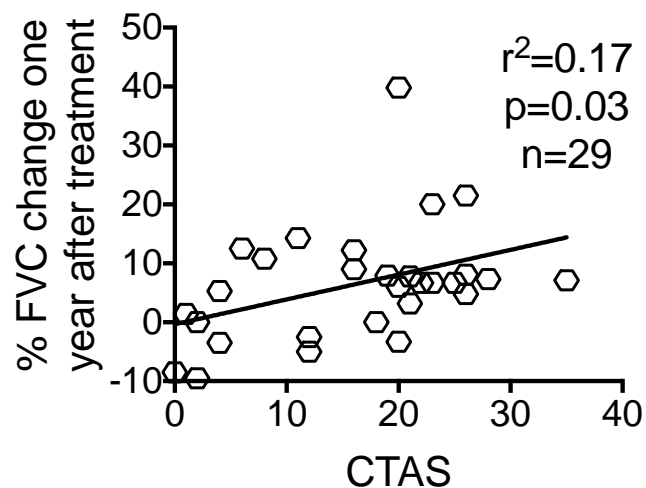
Acknowledgement

The study was funded by the NIHR Biomedical Research Centre at Oxford

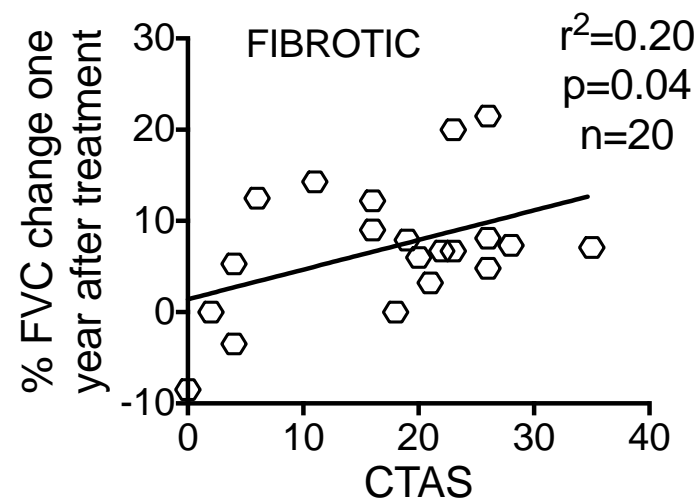
n	97
Age range (years)	24-79
Age mean (S.D.)	51 (13)
FEV1 Range	32-124%
FEV1 Mean (S.D.)	85 (20)%
FVC Range	37-135%
FVC Mean (S.D.)	98 (19)%
DLCO Range	26-139%
DLCO Mean (S.D.)	80 (21)%
Gender (F)	42 (44%)
Current smoker	8 (8%)
Afro-carribean	6 (6%)
Asian (sub-Indian continent)	3 (3%)
Scadding Stage 1/2/3/4	20/49/9/19
Lung involvement	97 (100%)
Skin involvement	8 (8%)
Liver involvement	7 (7%)
Cardiac involvement	7 (7%)
CNS involvement	2 (2%)
Bone involvement	2 (2%)
Eye involvement	10 (10%)

Table 1. Demographic data for patient cohort. Pulmonary function test refers to % predicted for age, gender and height. Unless stated, % in parentheses refer to % of cohort.

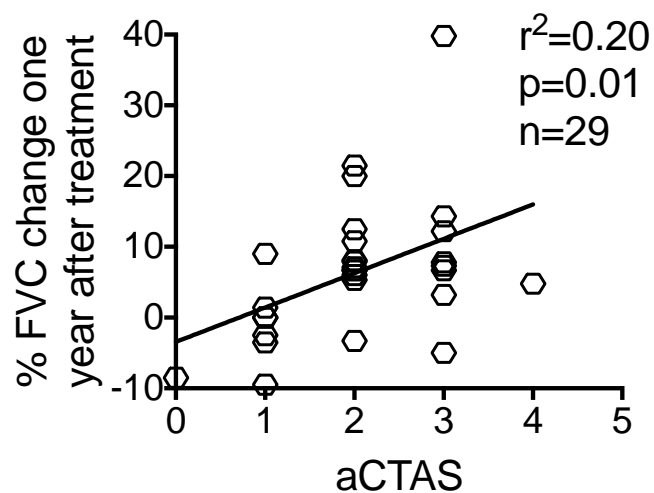
A.



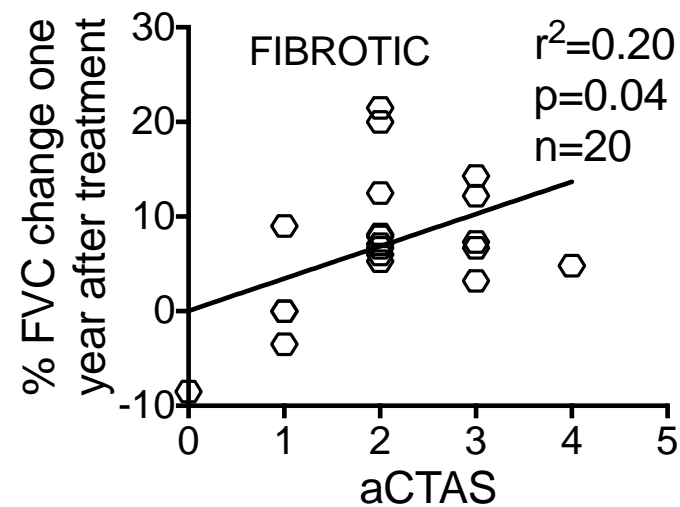
B.



C.



D.



1
2
3
4
5
6
7
8
9
10
11
12
13
14
15
16
17
18
19
20
21
22
23
24
25
26
27
28
29
30
31
32
33
34
35
36
37
38
39
40
41
42
43
44
45
46
47
48
49
50
51
52
53
54
55
56
57
58
59
60

SUPPLEMENTARY METHODS, REFERENCES AND TABLES

Patient cohort

Diagnostic criteria were as outlined in WASOG¹. All patients were followed up for one year to record change in treatment and lung function. The resultant cohort comprised 97 patients whose CT scans were analysed completely without any missing data. Patients were aged between 24 and 79 years, with an FVC range between 37-135% predicted. 91% were Caucasian and all but 8 had had tissue confirmation of non-caseating granuloma. In those who did not have histological confirmation, the clinical and radiographic findings were typical, and bronchoalveolar lavage (BAL) showed lymphocytosis (>15% of BAL cells), with no evidence of infectious agents on BAL or bronchial washes. None had upper lobe fibrosis; and antigen exposure questionnaires were negative. None of the patients presented with Löfgren's syndrome, although this was not excluded intentionally.

For the study to examine the correlation of CTAS and aCTAS to FVC change after treatment, we extracted patients who, at the point of HRCT scanning, went on to start or increase treatment specifically for their lung disease (n=31). Therapy was started because of presence of end organ dysfunction, deteriorating lung function and/or progressive changes on CT scan. Two patients were excluded because of the development of pulmonary embolism, a new diagnosis of lung cancer during the follow up period, and one because commencement of treatment was for neuro-sarcoidosis, leaving 29 patients. All patients received either Prednisolone at 0.4-0.5 mg/kg, or Azathioprine (n=1). FVC values at 12 months (\pm 8 weeks) after treatment were compared to pre-treatment.

HRCT protocol, lung function and serum markers

HRCT scans were acquired using a 64-detector row CT scanner (LightSpeed VCT XT; GE Medical Systems, Milwaukee, WI, USA). In patients under the age of 45 years, an inspiratory HRCT was acquired using 1.25mm slices every 10mm and an expiratory HRCT using 1.25mm slices every 30mm; images were reconstructed using a high spatial resolution algorithm. In patients over the age of 45 years, a volumetric scan was performed with 0.625mm slice thickness at an interval of 0.625mm. 2.5mm axial and 3mm coronal and sagittal images were reconstructed using a soft tissue kernel. 1.25mm HRCT images were also reconstructed from the raw data; 1.25mm expiratory HRCT images were acquired in the same way as in patients under 45 years. Intravenous contrast was not routinely used but was administered in several patients in whom malignancy was considered clinically at the time of the scan.

Pulmonary function tests were performed in one standard pulmonary function laboratory. Serum ACE levels were measured on the Konelab 30 chemistry analyser using a Buhlmann kit (Basel, Switzerland) in a clinical laboratory. Serum IL-2R levels were measured using the Bio-plex™ Luminex immunoassay (Bio-Rad, Hemel Hempstead, UK) according to the manufacturer's instructions.

Scoring methods for HRCT abnormalities

Each HRCT was reported systematically by a comprehensive proforma that included all CT abnormalities (including fibrotic changes). These scans were then specifically scored for the presence, character and extent of sarcoidosis-related HRCT abnormalities [ground glass opacification (GGO), interlobular septal thickening (IST), nodularity, conglomeration, consolidation and intra-thoracic lymphadenopathy] using pre-defined criteria from either the Fleischner Society glossary of terms or pre-defined criteria from

previous peer-reviewed publications²⁻⁴. Specifically, conglomeration, a CT feature over-represented in pulmonary sarcoidosis is not a Fleischner term but defined as a “large opacity >3cm surrounding and encompassing hilar bronchi and vessels”². Extent was estimated visually in each anatomically defined zones on the HRCT (Supplementary Table 3a-b); and measured by quartiles (25%) for GGO and consolidation, 2.5 cm intervals of short-axis diameter for conglomeration, number of nodules per zone (0-25 / 26-50 / >50), and numbers of IST (<=5 or >5) per image for each zone⁵. Sub-1mm nodules were scored as GGO since the distinction between innumerable sub-1mm nodules and GGO was demanding with current HRCT resolution.

As the number of nodules may not reflect the true extent of nodularity as this may be confounded by nodule size (e.g. twenty 10-mm nodules may reflect more extensive active disease than fifty 2-mm nodules). We therefore questioned if the extent of nodularity scored by 25% portions of involvement rather than number of nodules (as above) showed better correlation with our selected disease activity marker and lung function tests. A random subset of scans was examined (n=50). We found that these correlated strongly with each other (r=0.94; p<0.0001; Spearman rank sum test); and the original method of enumerating nodules per zone was used.

Fibrosis was defined as presence of any honeycombing, traction bronchiectasis, reticulation or intra-lobular linear opacities with or without architectural distortion or lobar volume loss. Evidence of pulmonary hypertension was increase in pulmonary artery diameter plus increased right heart pressures by echocardiography where a trace tricuspid regurgitation was also observed.

Scoring of the HRCT scans was performed by a Fellowship-trained Consultant Thoracic Radiologists based at a regional Thoracic Imaging Centre, with ten (RB) years experience in interpreting thoracic CT. To evaluate reproducibility of composite markers, the first 85 scans were selected for scoring by a second radiologist, EH who is also Fellowship-trained, with seven years experience, and based a district general hospital.

Statistical methods

Correlations between extent of CT abnormalities and lung function changes or disease activity variables were performed using Spearman's Ranked Correlation test. The predictive capability of the CT scores for treatment response was modeled with linear regression analysis. These statistical methods are shown within the text of the Results. Analysis was performed by a bio-statistician (ER) using the R statistical programming environment⁶ or GraphPad Prism. Agreement between radiologists was measured using Pearson's correlation and systematic discrepancies between the two scores were examined with Bland and Altman test.

Reference

1. Statement on sarcoidosis. Joint Statement of the American Thoracic Society (ATS), the European Respiratory Society (ERS) and the World Association of Sarcoidosis and Other Granulomatous Disorders (WASOG) adopted by the ATS Board of Directors and by the ERS Executive Committee, February 1999. *Am J Respir Crit Care Med*. 1999;160(2):736-55
2. Akira M, Kozuka T, Inoue Y, Sakatani M. Long-term follow-up CT scan evaluation in patients with pulmonary sarcoidosis. *Chest*. 2005;127(1):185-91.
3. Abehsera M, Valeyre D, Grenier P, Jaillet H, Battesti JP, Brauner MW. Sarcoidosis with pulmonary fibrosis: CT patterns and correlation with pulmonary function. *AJR American Journal of Roentgenology*. 2000;174(6):1751-7.

4. Hansell DM, Bankier AA, MacMahon H, McCloud TC, Muller NL, Remy J. Fleischner Society: glossary of terms for thoracic imaging. *Radiology*. 2008;246(3):697-722.

5. Walsh SL, Hansell DM. High-resolution CT of interstitial lung disease: a continuous evolution. *Seminars in Respiratory and Critical Care Medicine*. 2014;35(1):129-44.

6. R: A language and environment for statistical computing. R Foundation for Statistical Computing, Vienna, Austria (2013). URL <http://www.R-project.org/>.

Legends

Supplementary figure 1. **A.** Distribution of CTAS for the patient cohort (n=97). **B.** CTAS in non-fibrotic and fibrotic pulmonary sarcoidosis. p value measured by Mann-Whitney test. **C-D.** Correlation of CTAS with contemporaneous lung function in all patients. **F-G.** Correlation of aCTAS with contemporaneous lung function in all patients. r and p value measured by Spearman correlation test.

Supplementary figure 2. **A.** CT from a patient with CTAS=4. Axial HRCT image showing subtle foci of ground glass opacity in the left lower lobe and middle lobe (arrows). There is no other parenchymal abnormality. **B.** Patient with CTAS = 4. There is perihilar fibrosis with traction bronchiectasis. There are several small nodular opacities bilaterally. There is ground glass opacity in the lower zones (not shown) and lymphadenopathy. **C.** Patient with CTAS=7. There are several clusters of micronodules in both upper lobes. There is coalescence into larger denser nodules (arrow) and areas of consolidation (asterisk). **D.** A patient with a CTAS=16. There is bilateral peribronchovascular nodularity, which extends from apices to bases and is worse in the upper zones (i). There is right perihilar conglomeration (arrow) (ii). There is no consolidation, ground glass opacity or interlobular septal thickening. **E.** A patient with a CTAS = 20. There is widespread micronodularity and ground glass opacities. Micronodules coalesce into an area of consolidation in the right upper lobe (asterisk) (i). There is also interlobular septal thickening in the right middle and lower lobes (arrows) (ii). **F.** A patient with a CTAS = 58. There is diffuse ground glass opacity, micronodularity and interlobular septal thickening, with an area of consolidation in the right upper lobe (arrow) (i). The interlobular septal thickening is nodular and more marked in the lower zones (ii)

Supplementary figure 3. **A.** Agreement between two radiologists for CTAS. Pearson correlation analysis (n=85), and **B.** Bland Altman test. Mean differences (bias) of -0.4, and 95% limit of agreements (precision) (-8.5 to 7.7) are shown.

ABNORMALITY	PRESENCE	DESCRIPTION	EXTENT	
Ground glass opacity (GGO)	Y / N	Axial distribution in lung: central / peripheral / dorsal / ventral / diffuse / dependent / patchy Relation to secondary pulmonary lobule: random / peribronchovascular / subpleural / centrilobular	Extent (to nearest 25%) RUZ LUZ RMZ LMZ RLZ LLZ	
Consolidation	Y / N	Axial distribution in lung: central / peripheral / dorsal / ventral / diffuse / dependent / patchy Relation to secondary pulmonary lobule: random / peribronchovascular / subpleural / centrilobular Cavitation Y / N if yes: location (lobe)	Extent (to nearest 25%) RUZ LUZ RMZ LMZ RLZ LLZ	
Interlobular septal thickening (IST)	Y / N	Smooth / nodular	<=5 / >5 per image (if striking feature) RUZ LUZ RMZ LMZ RLZ LLZ	
Nodules	Y / N	Predominant size: <1mm / 1-3mm / 4-10mm, / >10mm Axial distribution in lung: central / peripheral / dorsal / ventral / diffuse / dependent Relation to secondary pulmonary lobule: random / bronchocentric / subpleural / centrilobular / tree in bud / perilobular margins: smooth / irregular cavitation: Y / N if yes: location (lobe)	Number of nodules per zone (0-25 / 26-50 / >50) RUZ LUZ RMZ LMZ RLZ LLZ Extent (to nearest 25%) RUZ LUZ RMZ LMZ RLZ LLZ	
Conglomeration	Y / N	In continuity with R hilum? Y / N L hilum? Y / N short axis dimension R: 0-2.5cm / 2.6-5cm / >5cm L: 0-2.5cm / 2.6-5cm / >5cm		
Lymphadenopathy	Y / N	Largest hilar: R (size+slice no) L (size+slice no) Largest mediastinal: R (size+slice no) L (size+slice no) calcification? Y / N If yes: amorphous / punctate / uniform / eggshell / popcorn (circle all that apply) associated bronchial narrowing? Y / N	if bronchial narrowing: RUL LUL RML Lingula RLL LLL	

Supplementary Table 1. Profoma of all relevant CT abnormalities for pulmonary sarcoidosis, and extent of the abnormalities. Definitions are found in Supplementary Table 2. Definition of zones are found in Table 1B. 'Central'- predominantly occupying inner 2/3 of the lung. 'Peripheral' - predominantly occupying outer 1/3 of the lung or along the inter-lobar fissures. 'Dorsal' - predominantly posterior portion of the lung. 'Ventral'- predominantly anterior portion of the lung. 'Dependent' -predominantly posterior portion of the lung with a relatively horizontal anterior margin.

Terms	Definition
Ground glass opacity	Hazy increased lung opacity, with preserved bronchial and vascular margins.
Consolidation	Homogeneous increase in pulmonary parenchymal attenuation which obscures vessels and airway walls.
Interlobular septal thickening	Thickening of the septa between lobules.
Traction bronchiectasis	irregular bronchial dilatation due to surrounding fibrosis
*Conglomeration	a large opacity >3cm surrounding and encompassing hilar bronchi and vessels

Supplementary Table 2. Definition of terms for abnormalities on HRCT. All from Fleischner Glossary of Terms apart from asterisked²⁻⁴.

A.

Abnormalities	Score for extent
GGO (or nodules <1mm)	One zone 1-25% = 1 point; one zone 26-50% =2; One zone 51-75%=3; one zone 76-100% = 4
Consolidation	One zone 1-25% = 1 point; one zone 26-50% =2;one zone 51-75%=3;one zone 76-100% = 4
Interlobular septal thickening	One zone, up to 5= 1 point; one zone >5 = 2
Nodules 1 mm or greater	One zone 1-25 nodules = 1 point; one zone 26-50 nodules = 2; one zone >50 nodules = 3
Conglomeration	Yes =1 point; no =0; each 2.5cm dimension (Right or Left) = 1
Lymphadenopathy	Yes =1 point; no =0

B.

Definition of zones on HRCT	
Upper zone	Predominantly above the carina in the cranio-caudal plane
Lower zone	Predominantly below inferior pulmonary veins in the cranio-caudal plane
Mid zone	Predominantly between UZ and LZ

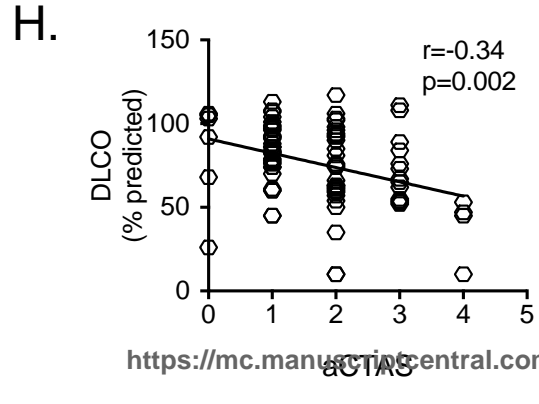
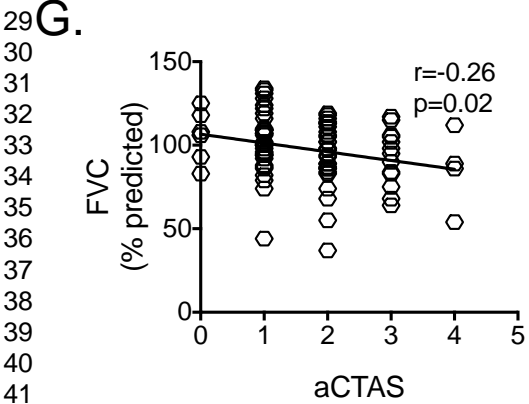
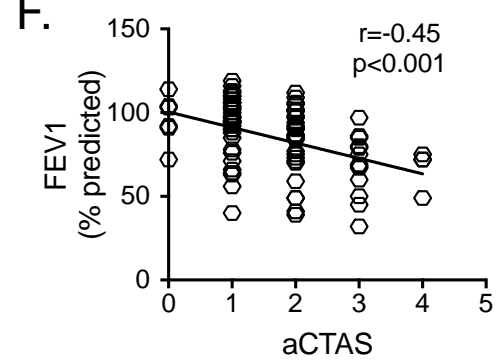
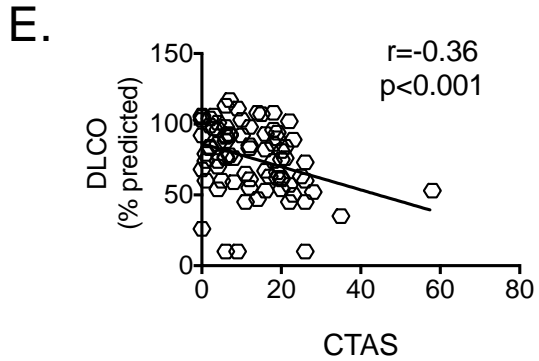
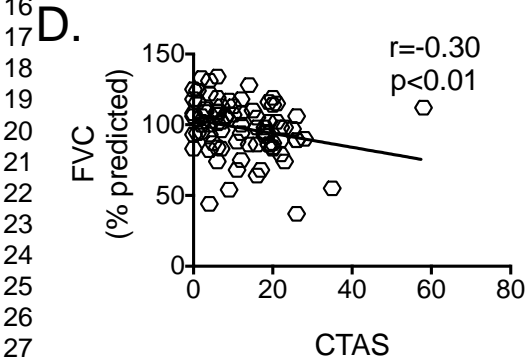
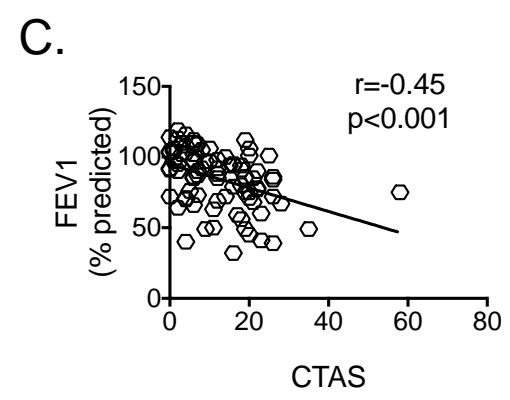
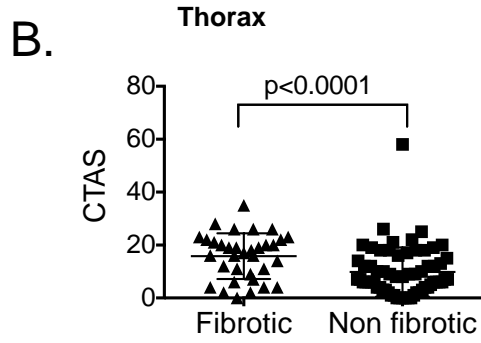
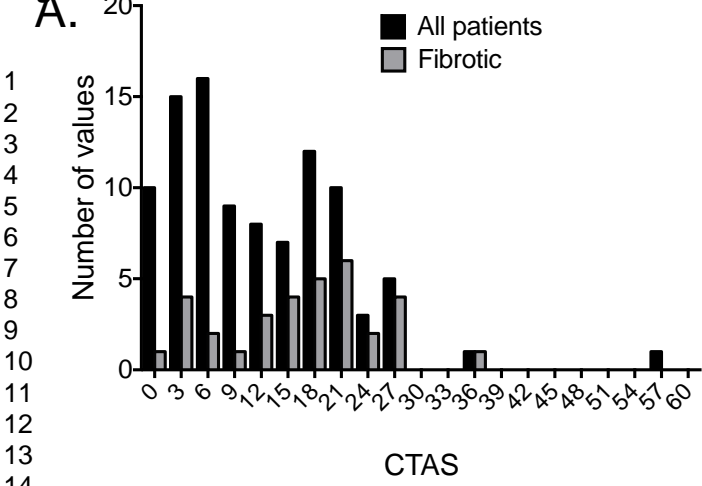
Supplementary Table 3. (A) Scoring system for HRCT abnormalities, and (B) definition of 'zones' used to measure extent. Other definitions for terms are found in Supplementary Table 1 and 2. GGO – ground glass abnormalities. Nodules that were sub-1mm were classified under GGO.

	Nodularity	GGO	Consolidation	ILT	Conglomeration
Range	0-18	0-24	0-6	0-12	0-4
Median (IQR)	6 (0-14)	0(0-2)	0(0-0)	0(0-2)	0(0-1)

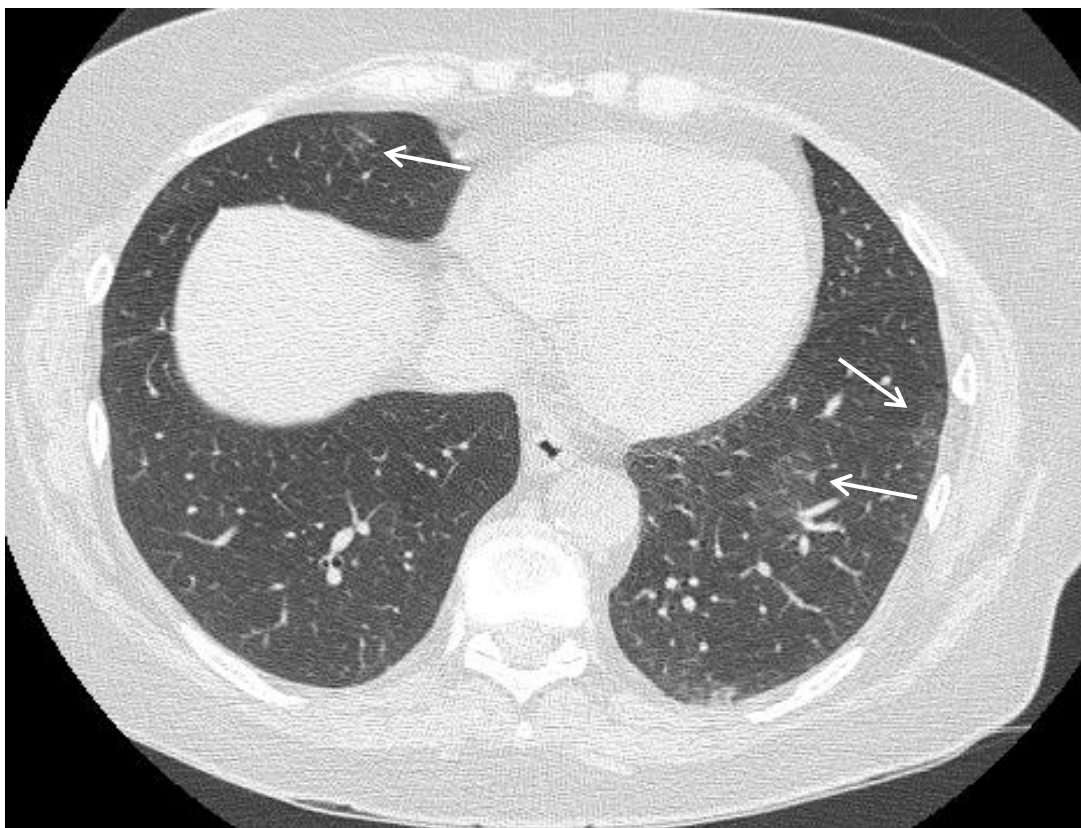
Supplementary Table 4. Range of CT abnormality extent scores in patient cohort

Correlation r (p value)	Nodularity	GGO	Consolidation	ILT	Conglomeration
sACE	0 (0.70)	*0.3 (0.01)	0.1 (0.52)	0.1 (0.40)	0 (0.91)
sIL2-R	*0.6 (0.01)	-0.4 (0.08)	-0.1 (0.77)	0.2 (0.49)	-0.3 (0.88)
Change in FVC	0.1 (0.40)	*0.3 (0.03)	*0.3 (0.03)	*0.3 (0.03)	0.3 (0.09)

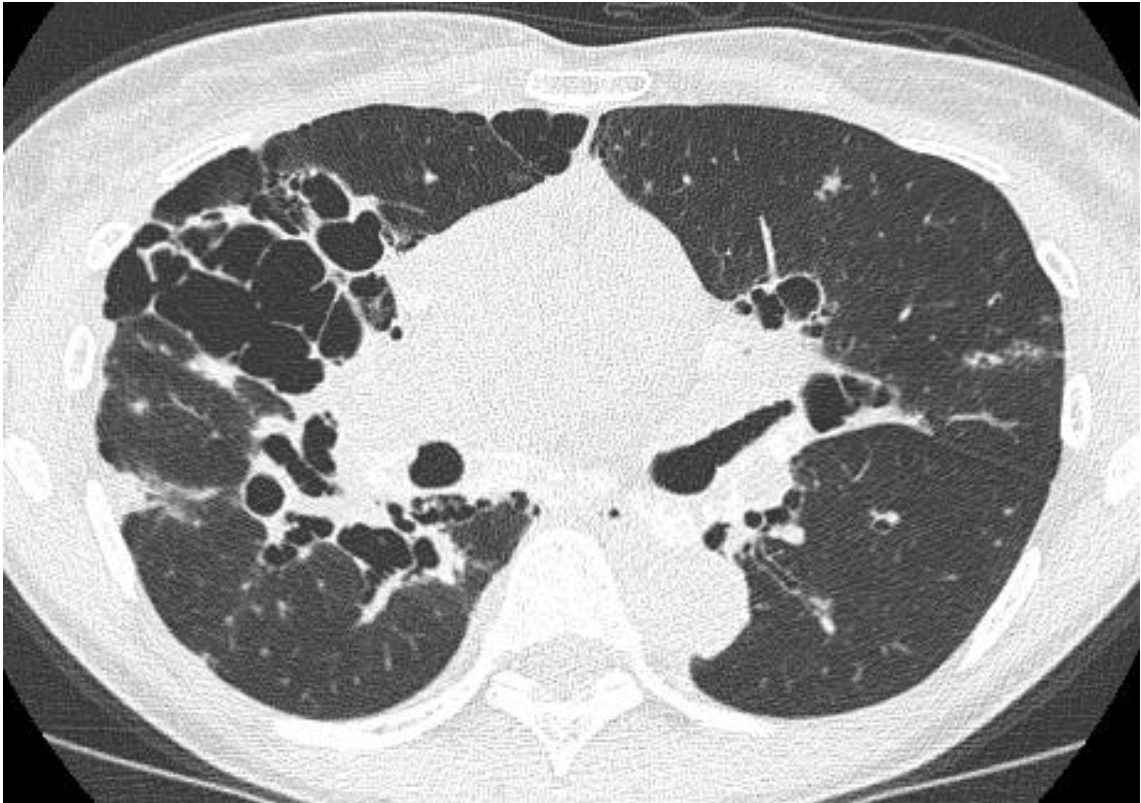
Supplementary Table 5. Correlation between disease activity surrogates and individual CT abnormalities. R and p value calculated using Spearman Rank Correlation test.



Supplementary Figure 1



A. A patient with CTAS=4. Axial HRCT image showing subtle foci of ground glass opacity in the left lower lobe and middle lobe (arrows). There is no other parenchymal abnormality.

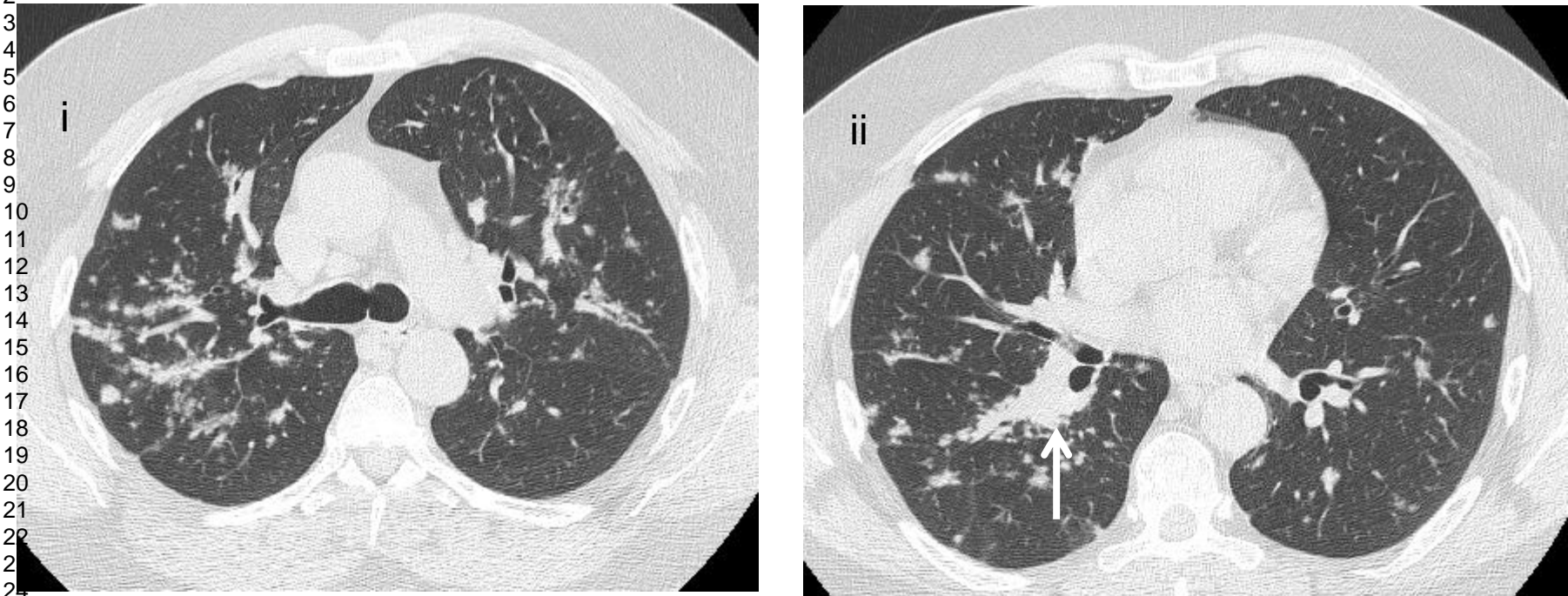


B. Patient with CTAS = 4. There is perihilar fibrosis with traction bronchiectasis. There are several small nodular opacities bilaterally. There is ground glass opacity in the lower zones (not shown) and lymphadenopathy.



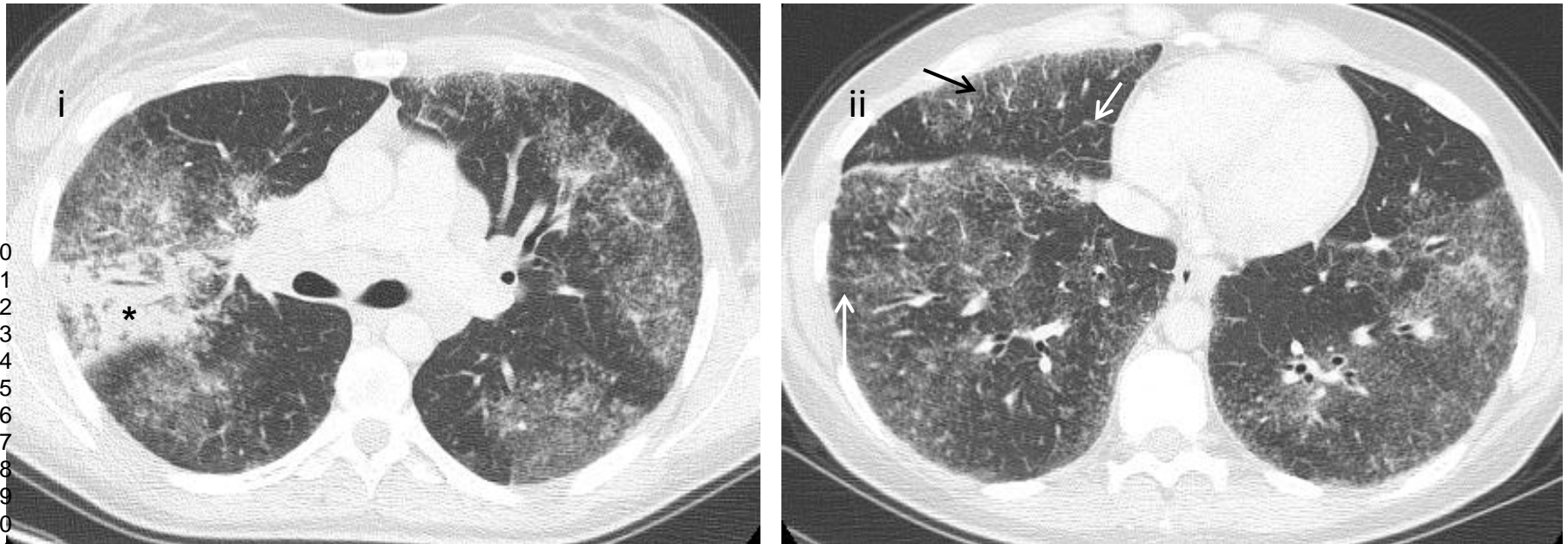
C. Patient with CTAS=7. There are several clusters of micro-nodules in both upper lobes. There is coalescence into larger denser nodules (arrow) and areas of consolidation (asterisk).

1
2
3
4
5
6
7
8
9
10
11
12
13
14
15
16
17
18
19
20
21
22
23
24
25
26
27
28
29
30
31
32
33
34
35
36
37
38
39
40
41
42
43



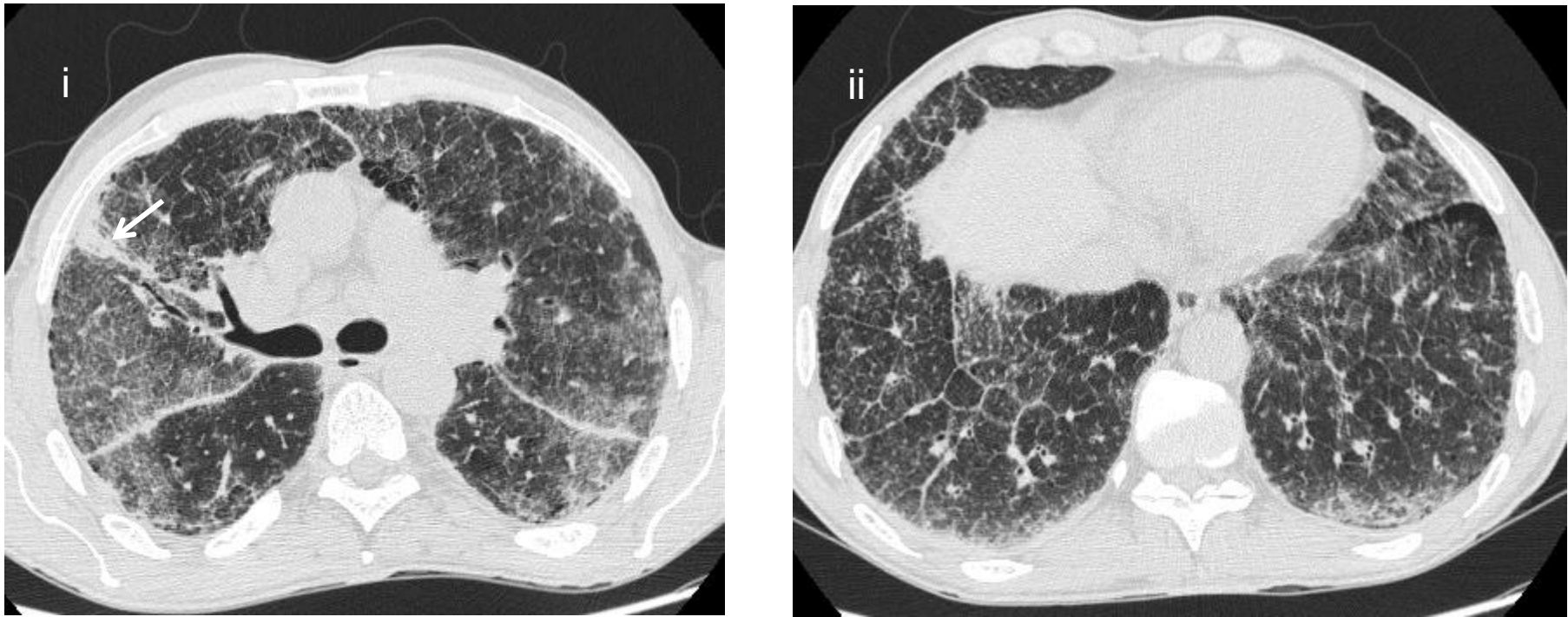
D. A patient with a CTAS=16. There is bilateral peribronchovascular nodularity, which extends from apices to bases and is worse in the upper zones (i). There is right perihilar conglomeration (arrow) (ii). There is no consolidation, ground glass opacity or interlobular septal thickening.

Supplementary Figure 2D



E. A patient with a CTAS = 20. There is widespread micronodularity and ground glass opacities. Micronodules coalesce into an area of consolidation in the right upper lobe (asterisk) (i). There is also interlobular septal thickening in the right middle and lower lobes (arrows) (ii).

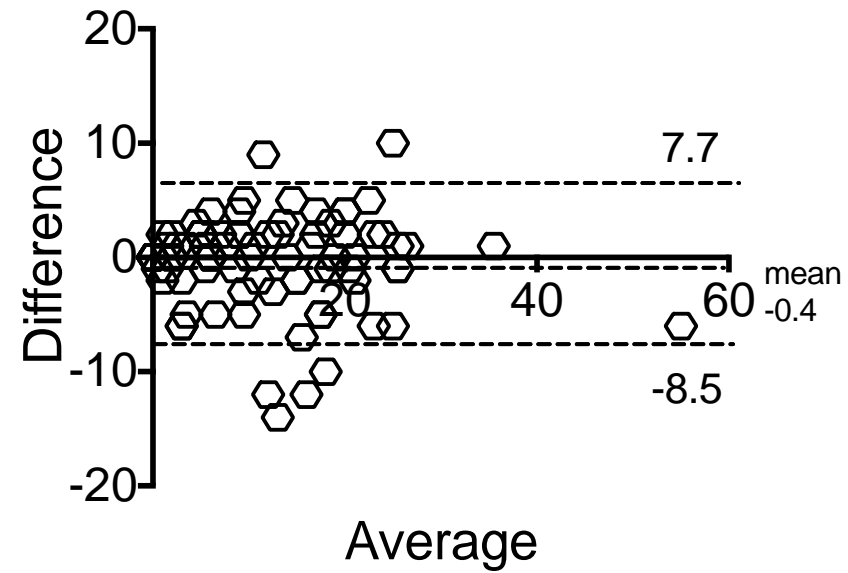
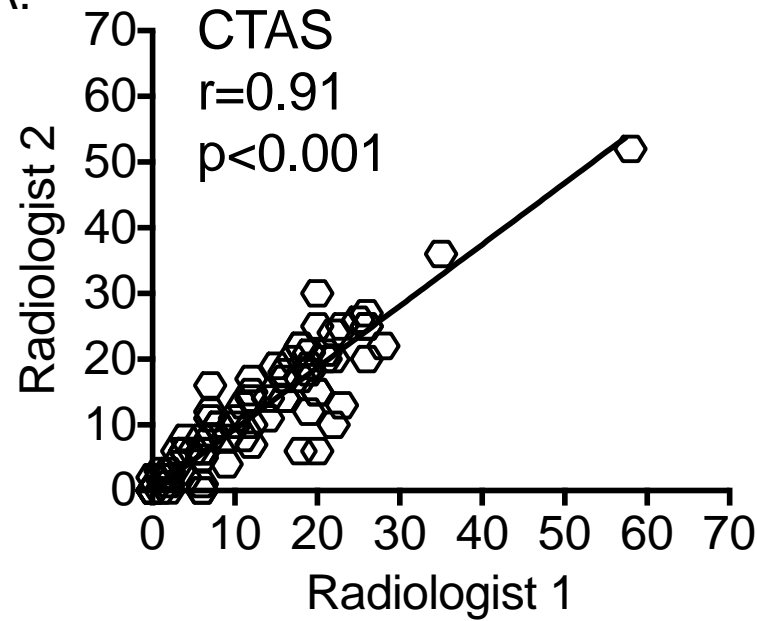
Supplementary Figure 2E



F. A patient with a CTAS = 58. There is diffuse ground glass opacity, micronodularity and interlobular septal thickening, with an area of consolidation in the right upper lobe (arrow) (i). The interlobular septal thickening is nodular and more marked in the lower zones (ii)

Supplementary Figure 2F

A.



Supplementary Figure 3